2019 International Conference on Robotics and Automation (ICRA)
Palais des congres de Montreal, Montreal, Canada, May 20-24, 2019

Design Principles and Optimization of a Planar Underactuated Hand for Caging Grasps

Walter G. Bircher, *Student Member, IEEE,* and Aaron M. Dollar, *Senior Member, IEEE*

Abstract— **In this paper we address the problem of creating planar caging grasps on objects using simple, underactuated grippers with no sensing or control. Specifically, we examine how changes in mechanical compliance, passive adaptability due to underactuation, and finger phalanx length affect the ability to create caging grasps passively, by altering the free-swing motion of the fingers. We present a simple model for simulating the underactuated hand, develop a metric for quantifying a hand design's caging ability, and perform a design parameter space search to reveal the important design factors influencing passive caging behavior. The results show that both palm width and the interplay between joint spring stiffness and pulley radius ratios play the largest roles in determining caging behavior. The effect of varying design parameters on the caging grasp performance of the hand is discussed, the best resulting design is shown, and a list of principles to guide the design of simple underactuated hands for caging grasps is presented.**

I. Introduction

Underactuated hands are particularly good at delicately grasping objects of unknown shape, size, and stiffness without complex control. This remarkable ability comes from their compliance and joint coupling—as the fingers begin to touch a target object, the forces generated at contact begin to influence the kinematic configuration of the hand. In this way, underactuated hands simply wrap around objects they are grasping, trading high forces at contact for large reconfiguration at the finger joints. But even before contact, the design features of the hand play an enormous role in determining the finger closing motions. By carefully tuning design parameters, we can produce hand closing motions that range from a stabbing-like behavior that ensures contact first occurs at the very end of the fingertips—to a passively occurring caging behavior on the other end of the spectrum. It is this idea that inspires our work, motivated also by the simplicity and accuracy of simulating this behavior. Essentially, the authors hope to show that through underactuation and intentional design choices, caging grasps can be made automatically over a wide range of objects by simply closing the hand. We hope that this work can be used as practical reference for the design of simple 'made-to-cage' robotic hands.

We narrow our scope to an underactuated hand model consisting of two 2-link fingers, each of which has a torsion spring and a pulley at each joint and a single tendon which drives both joints via their pulleys. Through simulation, we examine the effect of hand design parameters, including phalanx length, palm width, joint stiffness, and joint actuation torque on a hand's ability to create caging grasps over a wide range of object sizes and locations with respect to the hand's palm. We analyze the effect of varying these parameters on the planar caging performance for this simple underactuated hand model, considering both the workspace of object locations able to be caged as well as the "quality" of the cage, quantified by the ratio of the largest opening between the fingers, and the object diameter. The results lend insight into important design features of underactuated hands in terms of passively creating caging grasps.

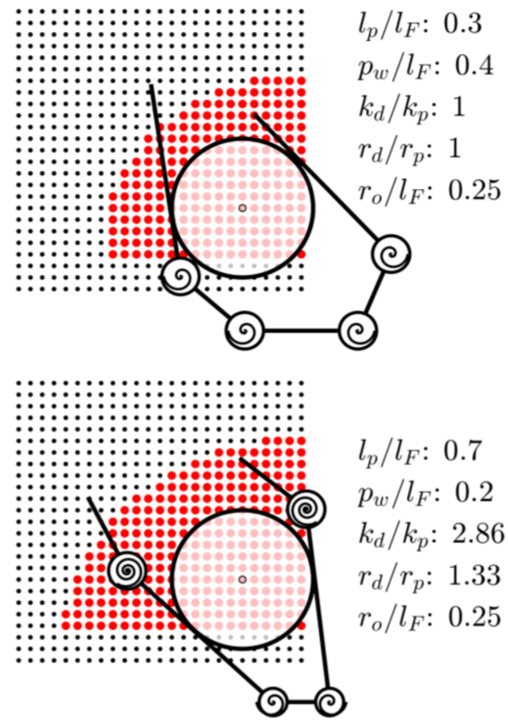

Figure 1. Design parameter selection determines the largest opening between the fingers at contact, the number of reachable object positions, and in turn the passive caging ability of a simple underactuated hand. Spring stiffness is illustrated by the number of coils, and pulley radius by the size of the joint.

We are not the first to consider the quality of a caging grasp. In particular, Sudsang et al. developed a cage quality metric for partial caging grasps, based on the probability of finding an escape path from a partial cage [1]. Similarly, Makita et al. developed a partial caging quality measure based on the likelihood of ejection, while considering the dynamics of the object [2]. All of this work is based on decades of

This work was supported in part by the National Science Foundation grants IIS-1317976 and IIS-0952856.

W.G. Bircher and A.M. Dollar are with the Department of Mechanical Engineering and Materials Science, Yale University, New Haven, CT 06511 USA, (e-mail: walter.bircher@yale.edu, aaron.dollar@yale.edu).

research into algorithmically generating caging grasps, immobilization, and studies of geometry. Ever since Besicovitch posed the challenge problem "A net to hold a sphere" to his students in 1957, a great amount of research has focused on 'caging' grasps and developing algorithms to find them [3]. In 1990, Kuperberg posed a number of problems helping to formalize the notion of caging, which he described as "immobilizing compact sets in the plane with points" [4], [5]. Rimon and Burdick developed another theory of immobilization and found geometric requirements for immobilizing planar objects [6], [7]. Wan et al. showed how caging could be used to guard against uncertainty during grasping [8]. Sudsang developed an algorithm capable of generating all possible caging sets for nonconvex polytopes [9], [10].

More closely related work focuses specifically on the design of hands for caging. Yoshida et al. created a quasi-static simulation of an underactuated finger closing around an object, and used it to design a two fingered underactuated gripper for more reliably grasping free-flying objects, by passively formed caging grasps [11]. Similarly, Backus designed an underactuated hand to "maximize the wrap of the digits about the object" for improving the robustness of aerial grasping and perching [12]. Other works comment on the particular ability of underactuated hands to passively create caging grasps [13], [14], [15], and many leverage design parameter optimization to produce desirable open-loop hand motions [16], [17], [18], [19], [21]. It is in this vein that the authors address this work.

The rest of this paper is organized as follows: Section II describes the simulation of a simple underactuated hand model. Section III shows results from the design space parameterization search, including the resulting gripper design that was found to passively cage the widest range of object sizes over the largest portion of its reachable workspace, and discusses design implications resulting from this work. Finally, Section IV presents a list of design principles to guide the design of future hands for caging grasps.

II. Underactuated Hand Simulation

We created a simple simulation to study the effect of design on the ability of underactuated hands to form caging grasps as they close around an object, placed at points on a grid in front of the hand. The following sections detail the assumptions and mathematical formulations used to model the motion of tendon driven underactuated hands, and the metrics used to quantify their ability to create caging grasps.

A. Underactuated hand model

This work focuses on a planar two finger underactuated hand, where each finger is tendon-driven and has a rigid proximal and distal phalanx. There are two single degree of freedom revolute joints on each finger, each of which has a torsional spring for passive-opening compliance and a pulley for torque transmission via a tendon. This hand model is very similar to a number of popularized underactuated hands, such as the SDM Hand [17] and the Yale OpenHand Model T42 [20]. A diagram of this hand model is shown in Fig. 2. We assume that our hand is symmetric, meaning the right finger is a mirror image of the left, and that the hand operates quasi-statically, meaning that it operates slowly enough that any

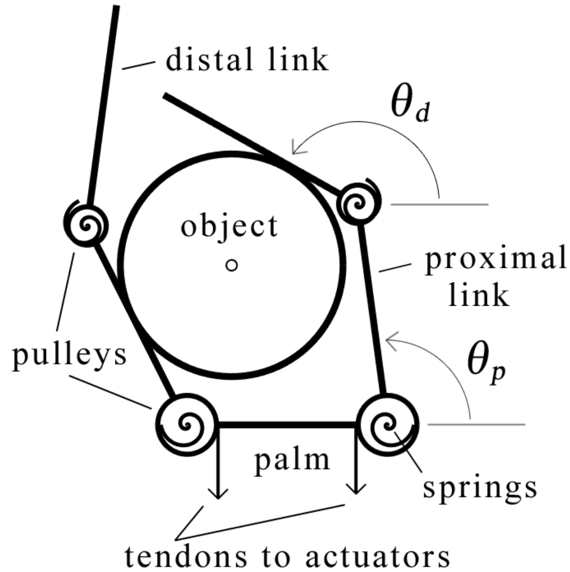

Figure 2. Design parameter selection determines the largest opening between the fingers at contact, the number of reachable object positions, and in turn the passive caging ability of a simple underactuated hand.

inertial effects can be ignored. Additionally, we assume that the hand operates in position control mode. This means that an actuator position is specified, which in turn shortens or lengthens each finger tendon accordingly, while letting the torque supplied to the actuator vary.

B. Free-swing trajectory simulation

While an underactuated finger is being closed and moving freely without any external loading, it behaves as a single degree of freedom mechanism. Specifically, all joints of the finger will move simultaneously and in a deterministic way such that the fingertip follows a single path through space, known as the free-swing trajectory. Conveniently, this path can be directly determined by the ratio of the torques at the joints of the finger. To see this, we must first realize that the tension in the tendon is constant throughout its length. This means that the applied torque at each joint is determined by the product of the tension and the radius of that joint's pulley—but in order for the finger to remain in static equilibrium, this torque must be balanced by the torsional spring at that joint. Thus, using knowledge of the pulley radii and torsional spring stiffness, we can easily compute the unloaded trajectory of an underactuated tendon-driven finger by writing an expression for moment balance about each joint.

$$\sum M = 0 \tag{1}$$

$$Tr_p - k_p(\theta_p - \theta_{rest}) = 0 \tag{2}$$

$$Tr_d - k_d(\theta_d - \theta_p) = 0 \tag{3}$$

$T, r_p, r_d, k_p, k_d, \theta_p, \theta_d, \theta_{rest}$ are tendon tension, proximal and distal pulley radius, proximal and distal spring stiffness, proximal and distal joint position, and the rest position of the proximal joint. It is assumed that a physical hard stop exists

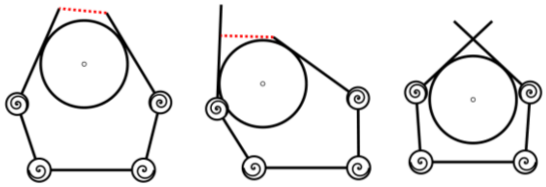

Figure 3. In this work, caging quality is defined as the length of the smallest opening between the fingers. This can either be the distance between the fingertips, the distance between a fingertip and opposing link, or zero if the fingers interdigitate.

that prevents the proximal joint from interfering with the palm of the hand, limiting its motion between 0 (θ_{rest}) and π radians. We also assume two hard stops on the distal joint, limiting the position to be between 0 and $\pi/2$ radians, relative to the proximal link. Recalling that the tendon tension is the same throughout its length, it can be eliminated from these equations, yielding the coupling ratio between the joints

$$T = \frac{k_p}{r_p}(\theta_p - \theta_{rest}) \tag{4}$$

$$T = \frac{k_d}{r_d}(\theta_d - \theta_p) \tag{5}$$

$$\frac{k_p}{r_p}\left(\theta_p - \theta_{rest}\right) = \frac{k_d}{r_d}(\theta_d - \theta_p) \tag{6}$$

$$\theta_d = \frac{k_p r_d}{k_d r_p}\left(\theta_p - \theta_{rest}\right) + \theta_p \tag{7}$$

From (7), it is clear that given a proximal joint angle, a corresponding free-swing distal joint angle θ_d can be automatically determined, based on the design parameters of the hand: r_p, r_d, k_p, k_d and θ_{rest}. Since we know the hard stop position of the proximal joint and all of the other design parameters, we simulate a range of proximal joint angles and calculate a corresponding range of distal joint angles, based on (7). Then, we can determine the paths that the links of the finger will follow as its tendon is shortened, yielding the path of its fingertip—the free-swing trajectory. Finally, if we know the object's position relative to the hand, we can determine the configuration of the fingers at the instant contact is made, under the simplifying assumption that the fingers do not perturb the object upon contact. We find each finger configuration at contact by simulating ever-increasing proximal joint angles starting from the finger's rest position, as if the finger is being actuated by pulling the tendon, until a link of the finger intersects the object, and contact is made.

C. Cage quality

Quantifying the quality of the cage is important because underactuated hands can reconfigure due to external disturbances, risking object ejection. A slight reconfiguration of the hand is more likely to break a looser cage than a tighter one. Thus, a tighter cage creates a more reliable grasp in the face of potential contact with other objects in the environment. In order to compare different hand designs against one another, we devised a metric based on both the tightness of caging grasps, as well as the number of object starting locations over which a caging grasp can be achieved. To construct our metric, we first determine the "quality" of a cage by computing the ratio of the largest possible opening between the fingers through which a contacted object could escape, and the diameter of the object being grasped. By this ratio, a cage of quality 1 is the minimum cage that can exist—any slight increase in the distance between the fingers breaks the cage. Conversely, a cage of quality 0 is an excellent cage—this occurs when the fingers leave no opening for the object to escape. Thus, a smaller opening between the fingers yields a higher quality cage. The length of this opening can be determined as either the distance between the fingertips, the normal distance between a fingertip and opposing link, or zero if the fingers completely cage the object via interdigitation (when the fingers mesh with one another). Examples of caging scenarios are shown in Fig. 3.

In addition to the quality of cage, we are also interested in the number of initial object positions from which the object can be caged by simply closing the hand, which we refer to as n_c. Ideally, we would like the initial caging capture region to be as large as possible to guarantee a successful initial cage in the face of large environmental uncertainty. Thus, we simulate grasping an object over a grid of starting positions in front of the hand (Fig. 1). Note that because our hand model is symmetric, we only need our grid to cover half of the area in front of the hand. Any result that we find for the left half will simply be mirrored on the right. Moving the object throughout our grid, we determine where it can be caged and compute the resulting quality, and count the total number of grid positions where a cage can be achieved for a given hand design. Finally, we can fully construct our metric, which we call the total cage score c_T. The total cage score for a single hand design is computed in the following way

$$c_T = \frac{1}{n_o}\sum_{n_o,n_c}\left(1 - c_q\right) \tag{8}$$

where c_q is the cage quality (the ratio of the largest finger opening and the diameter of the object being grasped) achieved at a single object starting point within the grid. This term is computed for each grid point where a cage can be established ($c_q \leq 1$), and added to a running total for each hand for all valid caging positions n_c. Then, the metric for a single hand design is averaged over all object sizes n_o. Thus, the hand with the highest value of c_T is able to achieve a high number of quality caging grasps.

D. Design parameterization

To examine the influence of design on a hand's ability to passively create a caging grasp, we parameterized our simulated hand model so that we could vary proximal and distal joint pulley radius, proximal and distal joint spring stiffness, proximal and distal link lengths, object diameter, and palm width. In order to reduce the size of our design space to decrease computation time, we held the total finger length constant while varying the distal link length. We did the same with spring stiffness and pulley radius, holding the proximal values constant in both cases, while varying the distal values—this works because the proximal to distal ratios affect the free-swing trajectory, rather than the values of the individual components (7). Also, we assumed hand symmetry and gave both the right and left fingers identical parameters.

Next, we discretized each of these parameters over a wide range of values, shown in Table I.

This enabled us to create 40,000 hand designs, which we scored with our metric (8). Each hand's metric was averaged over a range of object radii (last row of Table I). In this way we were able to compare the caging ability of underactuated hands over a wide swath of design space, caging a large range of object sizes. The total cage scores for 3,600 hands are shown in Fig. 4.

TABLE I. DESIGN PARAMETER VARIATION

Parameter	*Min*	*Max*	*Resolution*
r_p – proximal pulley radius	0.10		1
r_d- *distal pulley radius*	0.075	0.15	10
k_p – *proximal spring stiffness*	0.025		1
k_d – *distal spring stiffness*	0.01	0.10	20
l_p – *proximal link length*	0.10	0.90	20
l_d – *distal link length*	$1 - l_p$		20
p_w – *palm width*	0.05	0.70	10
r_o – *object radius*	0.15	0.30	10

All values are proportional to a unit length, and not physical units. In the case of stiffness, only the proximal and distal ratio is important, so units cancel out.

III. Design Parameterization Results

Parameter selection is a delicate balancing act. As shown in Fig. 4, each design parameter has considerable influence over the final result. The following sections detail the effects of each specific category of design features.

A. Effect of link lengths and palm width

The effect of changing link lengths is most pronounced when the palm of the hand is very small. This is because when the palm is small the proximal links of the hand tend to make first contact with the object, leaving the fingertips spread wider apart as the distal springs get stiffer. This is why the best regions of the first row of Fig. 4 have much lower spring stiffness ratios than the overall best results on row 2. Overall, variation in palm size produces some of the most striking differences across Fig. 4. The fact that row 2 contains the best results suggests that there is a palm size that is "just right" (not too large, not too small), for a fixed finger length. This is because when the palm grows too large, fixed length fingers can no longer reach objects on the far ends of the grid, reducing the number of grid positions where a cage can be achieved.

B. Effect of spring stiffness ratio and pulley ratio

As predicted by its role in calculating the free-swing trajectory (7), the ratio of spring stiffness is central in determining a hand's success in creating a natural caging behavior. The role of spring stiffness is perhaps most evident

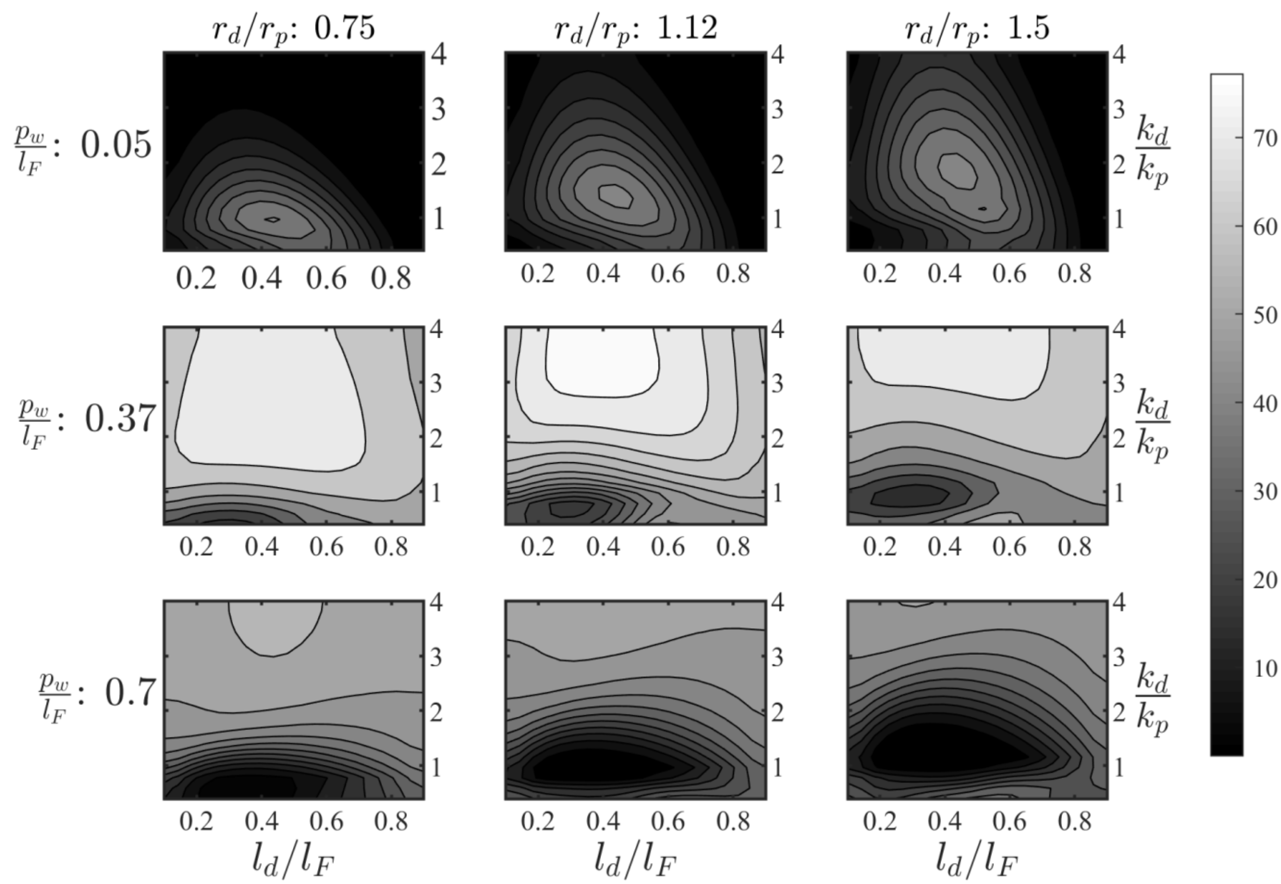

Figure 4. Results of the design parameterization shows a range of caging ability (lighter is better) while varying link lengths, palm width, joint stiffness, and pulley radius. Each point represents the performance of a single hand design over its entire reachable workspace, averaged over the full range of object sizes. The lighter the color, the more high quality caging grasps a hand can make, based on the metric in (8).

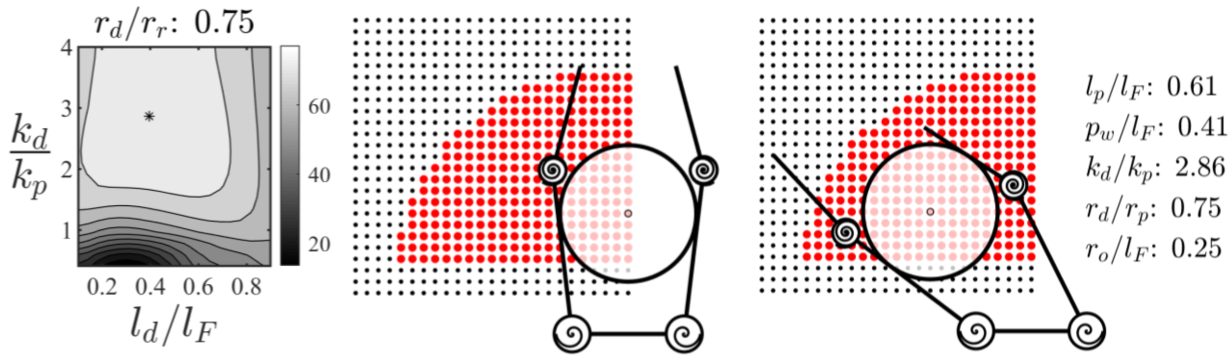

Figure 5. Left: The slice of design space containing the best gripper; Center & Right: The best gripper and its design parameters.

in the center subplot in Fig. 4, as it shows that improper spring selection makes the difference between some of the best grippers shown in the entire grid of subplots and some of the worst. This is because the middle column of subplots has a pulley radius ratio that is nearly equal to one. Indeed, looking at (7), when r_p and r_d are equal, the scaling of the distal joint travel relative to the proximal travel is entirely determined by the ratio of spring stiffnesses. Thus, the effect of changing spring stiffness is most amplified by similar pulley radii. The same can be said for spring stiffness ratios near one, which increases the influence of pulley ratio. These two ratios must be chosen with care, lest they cancel each other out.

C. *Best gripper for caging object acquisition*

The best gripper found by the search of the design space is shown in Fig. 5. The design parameters $r_p, r_d, k_p, k_d, l_d, l_p$, and p_w are equal to 0.1, 0.075, 0.025, 0.072, 0.394, 0.605, and 0.411, normalized to a unit length or stiffness. Its distal link is shorter than the proximal link, and its palm width is approximately the same length as the distal link. Its proximal pulley is larger than its distal pulley, and it has a stiffer distal spring than its proximal spring.

IV. Conclusion and Design Principles

In this paper we examined the influence of design on the passive caging ability of underactuated hands through extensive simulation. Interpreting the results from Fig. 4, we can write a list of principles that can help to guide the design of future underactuated hands, for maximal caging ability.

1. Caging ability suffers when the palm is either too small or too large
2. Large palms make it more difficult for both fingers to reach objects that are off center of the hand
3. Small palms result in proximal-link-first contact, pushing the object away
4. In the case of a small palm, special attention should be given to both the pulley radius ratio and stiffness ratio to ensure the distal links close in quickly enough to cage the object
5. Pulley ratio and stiffness ratio complement each other—and the effect of either is amplified when the other is close to unity (see (7))

In short, if you are designing a hand for better caging performance, select design parameters that follow these principles, or are found in a bright region of Fig. 4 for best results.

References

[1] Makapunyo, T., Phoka, T., Pipattanasomporn, P., Niparnan, N., & Sudsang, A. (2013, May). Measurement framework of partial cage quality based on probabilistic motion planning. In Robotics and Automation (ICRA), 2013 IEEE International Conference on (pp. 1574-1579). IEEE.

[2] Makita, Satoshi, and Kazuyuki Nagata. "Evaluation of finger configuration for partial caging." Robotics and Automation (ICRA), 2015 IEEE International Conference on. IEEE, 2015.

[3] Besicovitch, Abram Samoilovitch. "A net to hold a sphere." The Mathematical Gazette 41.336 (1957): 106-107.

[4] Kuperberg, Wlodzimierz. "Problems on polytopes and convex sets." DIMACS Workshop on polytopes. 1990.

[5] O'Rourke, Joseph. "Computational geometry column 18." ACM SIGACT News 24.1 (1993): 20-25.

[6] Rimon, Elon, and Joel W. Burdick. "Mobility of bodies in contact. I. A 2nd-order mobility index for multiple-finger grasps." IEEE transactions on Robotics and Automation 14.5 (1998): 696-708.

[7] Rimon, Elon, and Andrew Blake. "Caging planar bodies by one-parameter two-fingered gripping systems." The International Journal of Robotics Research 18.3 (1999): 299-318.

[8] Wan, W., Fukui, R., Shimosaka, M., Sato, T., & Kuniyoshi, Y. (2012, May). Grasping by caging: A promising tool to deal with uncertainty. In Robotics and Automation (ICRA), 2012 IEEE International Conference on (pp. 5142-5149). IEEE.

[9] Sudsang, Attawith, Jean Ponce, and Narayan Srinivasa. "Algorithms for constructing immobilizing fixtures and grasps of three-dimensional objects." (1997).

[10] Pipattanasomporn, Peam, and Attawith Sudsang. "Two-finger caging of nonconvex polytopes." IEEE Transactions on Robotics 27.2 (2011): 324-333.

[11] Hirano, Daichi, Kenji Nagaoka, and Kazuya Yoshida. "Design of underactuated hand for caging-based grasping of free-flying object." System Integration (SII), 2013 IEEE/SICE International Symposium on. IEEE, 2013.

[12] Backus, Spencer B., Lael U. Odhner, and Aaron M. Dollar. "Design of hands for aerial manipulation: Actuator number and routing for grasping and perching." Intelligent Robots and Systems (IROS 2014), 2014 IEEE/RSJ International Conference on. IEEE, 2014.

[13] Balasubramanian, Ravi, Joseph T. Belter, and Aaron M. Dollar. "Disturbance response of two-link underactuated serial-link chains." Journal of Mechanisms and Robotics 4.2 (2012): 021013.

[14] Odhner, Lael U., et al. "A compliant, underactuated hand for robust manipulation." The International Journal of Robotics Research 33.5 (2014): 736-752.

[15] Ma, Raymond R., Walter G. Bircher, and Aaron M. Dollar. "Toward robust, whole-hand caging manipulation with underactuated hands." Robotics and Automation (ICRA), 2017 IEEE International Conference on. IEEE, 2017.

[16] Spanjer, Stefan AJ, et al. "Underactuated gripper that is able to convert from precision to power grasp by a variable transmission ratio." Advances in Reconfigurable Mechanisms and Robots I. Springer, London, 2012. 669-679.

[17] Dollar, Aaron M., and Robert D. Howe. "The highly adaptive SDM hand: Design and performance evaluation." The International Journal of Robotics Research 29.5 (2010): 585-597.

[18] Bircher, Walter G., Dollar, Aarom M., and Rojas Nicolas. "A two-fingered robot gripper with large object reorientation range." Robotics and Automation (ICRA), 2017 IEEE International Conference on. IEEE, 2017.

[19] Laliberté, Thierry, Lionel Birglen, and Clement Gosselin. "Underactuation in robotic grasping hands." Machine Intelligence & Robotic Control 4.3 (2002): 1-11.

[20] Ma, Raymond R., & Dollar, Aaron M. Yale OpenHand Project: Optimizing Open-Source Hand Designs for Ease of Fabrication and Adoption. IEEE Robotics & Automation Magazine, (2017): 24(1), 32-40.

[21] Aukes, Daniel M., Barrett Heyneman, John Ulmen, Hannah Stuart, Mark R. Cutkosky, Susan Kim, Pablo Garcia, and Aaron Edsinger. "Design and testing of a selectively compliant underactuated hand." The International Journal of Robotics Research 33, no. 5 (2014): 721-735.